

## Report

# Physiological effects of ultrasound mist on fibroblasts

Jengyu Lai, DPM, and Mark R. Pittelkow, MD

From the Department of Dermatology,  
Mayo Clinic College of Medicine, Rochester,  
Minnesota

### Correspondence

Mark R. Pittelkow, MD  
Department of Dermatology  
Mayo Clinic  
200 First Street South-west  
Rochester, MN 55905  
E-mail: pittelkow.mark@mayo.edu

### Abstract

**Background** Chronic wounds present an increasing challenge in healthcare and consume a substantial portion of healthcare cost. Although new treatments have been developed, treatment success has not been improved greatly. Ultrasound has long been employed in medicine. Its unique ability to deliver energy makes it an ideal candidate as a wound care modality. We proposed that ultrasound would differentially affect intracellular signaling pathways and, with the ability to assess this effect using a noncontact form of ultrasound, were provided with a means to test this proposal.

**Methods** The cellular morphology, mitogenic activities, expression of keratinocyte growth factor (KGF) and transforming growth factor  $\beta$ -1 (TGF- $\beta$ 1), and activation of extracellular regulated kinase (ERK) and c-Jun N-terminal kinase (JNK) signaling pathways of dermal fibroblasts were studied after ultrasound treatment. Untreated and scrape-wounded fibroblasts were utilized as controls.

**Results** There was no difference in morphology observed, except for vacuolization in ultrasound-treated fibroblasts. Mitogenic activities were similar between ultrasound-treated and scrape-wounded fibroblasts. Ultrasound-treated fibroblasts exhibited a much earlier increase in KGF expression, ERK activation, and JNK activation. The ERK/JNK ratio was increased markedly in ultrasound-treated fibroblasts.

**Conclusion** We conclude that ultrasound induces cellular responses that may be beneficial to wound healing.

### Introduction

An estimated 2% of the American population suffers from chronic wounds, resulting from diabetes mellitus, venous insufficiency, and excessive pressure. According to the American Diabetes Association and other studies, diabetes mellitus is the sixth leading cause of death, and the medical cost for diabetic care ranges from \$98 to \$113 billion per year.<sup>1-7</sup> It is estimated that 15% of patients with diabetes have foot ulcers, and that one in 150 patients with diabetes has an amputation. In addition, more than 50% of nontraumatic lower limb amputations, nearly 82,000 new amputations, are in the diabetic population each year. Approximately 84% of amputations begin as a simple ulcer. More significantly, 30-50% of amputation patients undergo further amputation of the remaining lower extremity within 5 years, with a 50% mortality rate.<sup>6,8</sup> It is estimated that 1-1.2% of the population in the USA suffers from venous stasis ulcers.<sup>9</sup> Both forms of chronic ulcer compromise a patient's ability to ambulate, cause pain and mental depression, and cost billions of dollars in healthcare. New treatment modalities are constantly being developed and refined.<sup>10,11</sup>

Ultrasound delivers energy through a pressure field generated by the transducer and causes the molecules of its transmission medium to oscillate or vibrate. Ultrasound is used both therapeutically and diagnostically in medicine. Ultrasound has been shown to accelerate wound healing, and several mechanisms have been suggested.<sup>12,13</sup> Ultrasound activates inflammatory cells, resulting in wound debridement and the production of chemical mediators, which activate fibroblasts.<sup>14,15</sup> This activation leads to the earlier accumulation of endothelial cells in tissues and the promotion of collagen synthesis via the stimulation of calcium influx, alteration of membrane permeability, and enhancement of fibroblast proliferation.<sup>14-18</sup> In addition, collagen deposited after ultrasound treatment is stronger and better organized.<sup>15,19-24</sup> Not surprisingly, tissue treated with ultrasound progresses through the phases of healing more rapidly.<sup>15</sup>

Chemical mediators produced after ultrasound treatment include tissue growth factors, which, in turn, mediate the activation of intracellular signaling pathways.<sup>25-29</sup> In addition, mechanical stimulation of cellular membranes occurs during the process of energy delivery. At least part of the signal transduction pathway that mediates responses to forces is

attributable to the adapter protein, Shc. Transduction of the Shc-mediated signal is coupled to the activation of extracellular signal-regulated kinases (ERKs) and c-Jun N-terminal kinase (JNK), which, in turn, regulate downstream transcription factors and nuclear events linked to specific cell responses.<sup>30,31</sup> We have shown that the epidermal growth factor (EGF) ligand–receptor system is the primary receptor tyrosine kinase signaling pathway in keratinocytes that regulates epidermal keratinocyte proliferation, differentiation, and cell survival following oxidative stress.<sup>32–36</sup> Moreover, we have recently demonstrated that the Shc adapter protein complex is specifically phosphorylated in response to cell survival signals triggered following EGF receptor activation by ligand.<sup>32–34</sup> In addition to the ERK and JNK signaling pathways, which have been shown to be functional cascades in keratinocytes, the other main family of mitogen-activated protein kinases (MAPKs) present in keratinocytes is the p38 kinase members. We have demonstrated previously that the ERK, JNK, and p38 kinase pathways are expressed, and that the activation of these pathways is coordinately regulated by keratinocytes in response to growth factor-mediated or stress-induced stimuli.<sup>32–35,37</sup> We hypothesized that ultrasound treatment would induce the activation of both ERK and JNK. As the balance of ERK and JNK may predict the fate of the cell, we examined the ERK/JNK ratios following ultrasound treatment of cell cultures.

## Materials and Methods

Normal dermal fibroblasts were isolated from neonatal foreskin and maintained in Dulbecco's modified Eagle's medium (DMEM) containing 10% fetal bovine serum. Cells were seeded at 70–80% confluence on six-well plates for protein studies, 24-well plates for mitogenic studies, 100-mm<sup>2</sup> plates for RNA studies, glass slides for scanning electron microscopy (SEM), and Aclar for transmission electron microscopy (TEM).

The ultrasound mist was applied 1.0 cm from the cell culture and delivered an energy of 0.002 W/cm<sup>2</sup>, according to the manufacturer's specifications. The duration of application was determined as the longest time during which the ultrasound mist did not dislodge cells from the plate surface. After the cell cultures had become confluent, a sterile saline mist was applied (30 s to 100-mm<sup>2</sup> plates, 15 s to six-well plates, and 7 s to 24-well plates) to the cells in a circular motion using a form of ultrasound at 40 kHz that is noncontact in nature, except for a fine mist that is created by the system evaluated (Celleration™, Eden Prairie, MN). As ultrasound mists may detach cells from the supporting surface, an *in vitro* cell scrape-wounded model and untreated fibroblasts were employed as controls. Wounding was created by making two intersecting scrapes on the cell cultures.

Fibroblasts were seeded on to glass slides for SEM and Aclar for TEM. Both types of slide were trimmed to fit six-well plates. Immediately, 2 h, and 1 day after ultrasound treatment, cells were

fixed and examined by the Electron Microscopy Core Facility (Mayo Clinic). Untreated cells served as controls.

For SEM, tissue was fixed in Trump's fixative (1% glutaraldehyde and 4% formaldehyde in 0.1 M phosphate buffer, pH 7.2).<sup>38</sup> Tissue was then rinsed for 30 min in two changes of 0.1 M phosphate buffer, pH 7.2. Some of the samples were postfixed for 1 h in phosphate-buffered 1% OsO<sub>4</sub>. This step was omitted in a third sample. After rinsing in two changes of distilled water for 30 min, tissue was dehydrated in progressive concentrations of ethanol to 100%, and either critical point dried or placed into Peldri™. All samples were mounted on aluminum stubs and sputter coated with gold/palladium. Images were captured on a Hitachi S4700 scanning electron microscope operating at 5 kV.

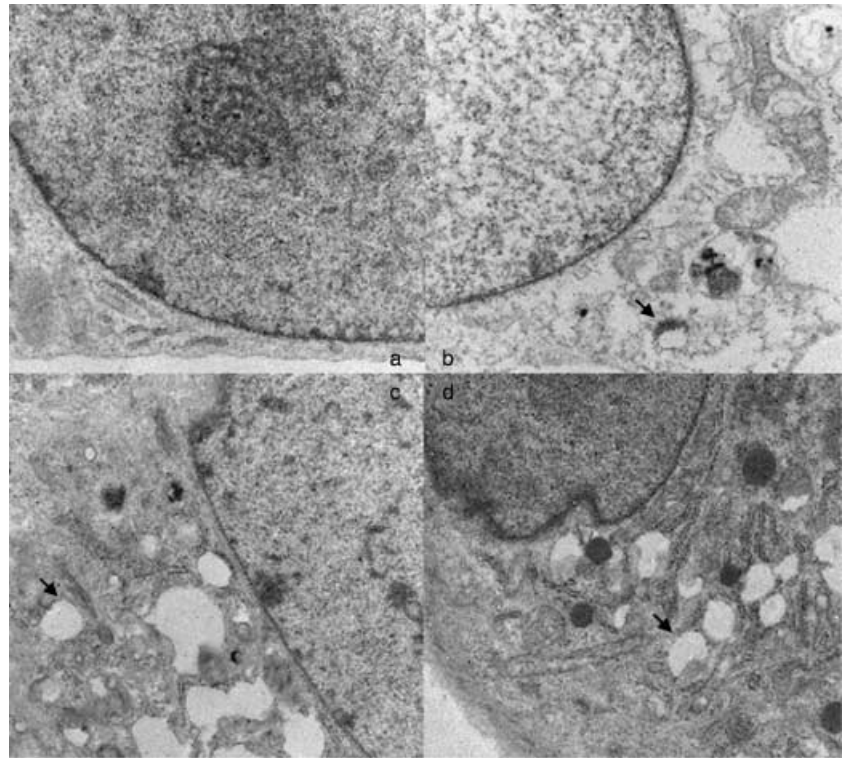
For TEM, tissue was fixed in Trump's fixative, and then rinsed for 30 min in three changes of 0.1 M phosphate buffer, pH 7.2, followed by a 1-h postfix in phosphate-buffered 1% OsO<sub>4</sub>. After rinsing in three changes of distilled water for 30 min, the tissue was *en bloc* stained with 2% uranyl acetate for 30 min at 60 °C. After *en bloc* staining, the tissue was rinsed in three changes of distilled water, dehydrated in progressive concentrations of ethanol and 100% propylene oxide, and embedded in Spurr's resin.<sup>39</sup> Thin (90-nm) sections were cut on a Reichert Ultracut E ultramicrotome, placed on 200-mesh copper grids, and stained with lead citrate. Micrographs were taken on a JEOL 1200 EXII operating at 60 kV.

Two hours and 1, 2, 3, and 4 days after treatment, tritiated thymidine was added to the cells to assess DNA synthesis. Nonultrasound-treated and nonscrape-wounded fibroblast cultures were used as controls. Two hours before the end of the time period, 1 µCi/10 µL of tritiated thymidine per milliliter of medium was added to the cell culture plate. Cells were incubated for 2 h at 37 °C. The radioactive medium was aspirated and the cells were washed with cold 10% trichloroacetic acid and rinsed with water. All liquid drops were carefully aspirated. This was followed by the addition of 0.2 mL of 0.2 M NaOH containing 40 µg/mL of herring sperm DNA to each culture plate. Cells were returned to the incubator for several hours, and 100 µL of liquid was taken in 3 mL of scintillation cocktail.<sup>40</sup>

Two hours and 1, 2, and 3 days after treatment, cells were extracted with TriZol (Life Technologies, Inc., Carlsbad, CA) for total RNA; 20 µg of total RNA from each sample was used for Northern blotting. Probes for keratinocyte growth factor (KGF), transforming growth factor β-1 (TGF-β1), and glyceraldehyde-3-phosphate dehydrogenase (GAPDH) were generated from plasmids. GAPDH was assessed for equal loading.

Two hours and 1, 2, 3, and 4 days after treatment, cells were extracted with MAPK lysis buffer for total proteins.<sup>41</sup> Extracts were heated at 100 °C for 5 min, loaded on to a 12% polyacrylamide gel for electrophoresis, and transferred to a membrane. The membrane was blotted against activated ERK 1/2 (Cell), total ERK (Santa Cruz Biotechnology, Santa Cruz, CA), and JNK (Cell Signaling, Beverly, MA). Total ERK was assessed for equal loading.

**Figure 1** Transmission electron microscopy. Fibroblasts were fixed after ultrasound treatment and observed under a transmission electron microscope: (a) untreated control; (b) immediately after treatment; (c) 1 h after treatment; (d) 1 day after treatment. Magnification:  $\times 50,000$ . Examples of vacuoles are indicated by arrows. The large dark organelles in the cytoplasm are lysosomes



The amounts of RNA in Northern blotting and protein in Western blotting were measured by the digital imaging software TotalLab (Phoretix, Durham, NC), and equal loading was calibrated on the basis of the amounts of GAPDH in Northern blotting and total ERK in Western blotting.

## Results

Samples were examined under SEM and TEM at various magnifications. No difference in the cell membrane was observed between the control and any treatment group (TEM data shown in Fig. 1; SEM data not shown); however, ultrasound-treated cells exhibited large vacuoles in the cytoplasm (Fig. 1b–d). As vacuoles are associated with the degradation of cellular proteins and macromolecules, we suspected that ultrasound waves mechanically stimulated the intracellular cytoskeleton and induced cellular remodeling.

DNA synthesis decreased 2 h after treatment, possibly related to limited cell detachment from the plate, and then increased significantly at days 1 and 2 and declined at day 3. No significant difference was observed between ultrasound-treated and scrape-wounded fibroblasts (Fig. 2), that is, ultrasound induced similar reparative activities to scrape-wounding.

Ultrasound-treated fibroblasts exhibited a marked increase in KGF expression shortly after treatment, but this decreased gradually. In contrast, fibroblasts in the wounding group

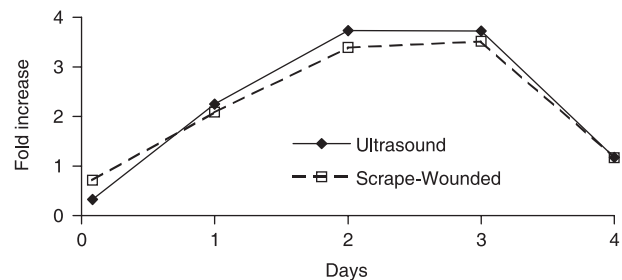


**Figure 2** Cellular DNA synthesis. Quiescent fibroblasts treated with tritiated thymidine incorporation assay. No difference was observed between ultrasound-treated and scrape-wounded fibroblasts

showed a decrease in KGF expression on the first day and a steady increase afterwards. TGF- $\beta$ 1 expression was elevated in ultrasound-treated fibroblasts in the first 2 days, and was decreased in wounded fibroblasts in the first 2 days (Fig. 3).

## ERK activation

Phospho-ERK expression in ultrasound-treated fibroblasts was markedly increased 2 h after treatment and returned to baseline on day 2; however, no significant changes in ERK activation over time were observed in wounded fibroblasts (Fig. 4).

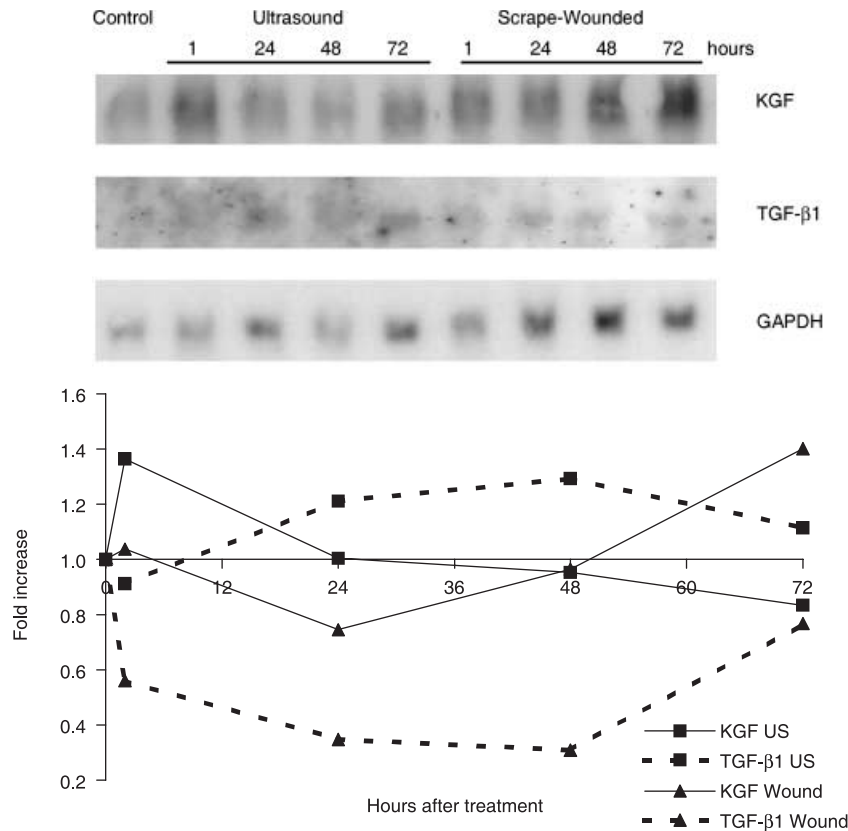


**Figure 3** Northern blotting. Total RNA was extracted from fibroblasts after ultrasound treatment (US) or scrape-wounding (Wound). The intensities of keratinocyte growth factor (KGF) and transforming growth factor  $\beta$ -1 (TGF- $\beta$ 1) were calibrated on the basis of glyceraldehyde-3-phosphate dehydrogenase (GAPDH)

### JNK activation

Phospho-JNK in ultrasound-treated fibroblasts was markedly increased at 2 h, but returned to baseline by day 2. Similarly, phospho-JNK was increased in wounded fibroblasts and returned to baseline on day 2 (Fig. 4). The substantial increase in phospho-JNK immediately after ultrasound treatment may result from the physical interactions of the ultrasound mist with cell membranes, as JNK is a member of the stress-activated kinase family.

### ERK/JNK ratio

The ERK/JNK ratio was increased on day 1 in ultrasound-treated fibroblasts; however, it was markedly decreased at 2 h and on day 1, and increased soon after, in wounded fibroblasts (Fig. 5). Ultrasound treatment enhanced the ERK-associated repair mechanism at day 1, whereas scrape-wounding only showed similar effects at days 2–4. The balance between ERK and JNK activation may regulate cell proliferation, growth arrest, and other cell repair and survival mechanisms.

### Discussion

It is common practice to debride chronic wounds and enhance healing by the removal of necrotic tissue, thus

converting a chronic wound to an acute state. Therefore, it would be expected that scrape-wounding would induce cell replication and repair. KGF specifically promotes the proliferation and migration of keratinocytes, rather than fibroblasts.<sup>42</sup> TGF- $\beta$  stimulates the regeneration of soft tissue and the production and deposition of collagen by fibroblasts.<sup>43,44</sup> Therefore, even though ultrasound treatment increased the production of KGF and TGF- $\beta$ , it produced a similar stimulation of fibroblast DNA synthesis to wounding.

Ultrasound treatment also increased the activation of both ERK and JNK, as had been proposed. Interestingly, the ERK/JNK ratios in ultrasound-treated and wounded fibroblasts exhibited opposite patterns; however, various downstream events, such as protein expression, that may be beneficial to wound healing were not measured. The cellular repair induced by ultrasound mist treatment is short term and distinct from cell wounding. This observation implies that ultrasound treatment may need to be applied at a frequency to optimize ERK activation, such as every 1–2 days. In addition, under these treatment conditions *in vitro*, JNK activation may indicate cellular stress that is not necessarily linked to apoptosis and cell death, but rather to compensatory responses mediating cellular repair. Further investigations on dose-dependent energy delivered to cells and the influx of calcium

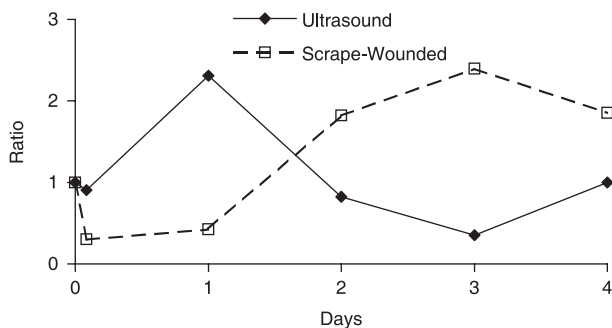
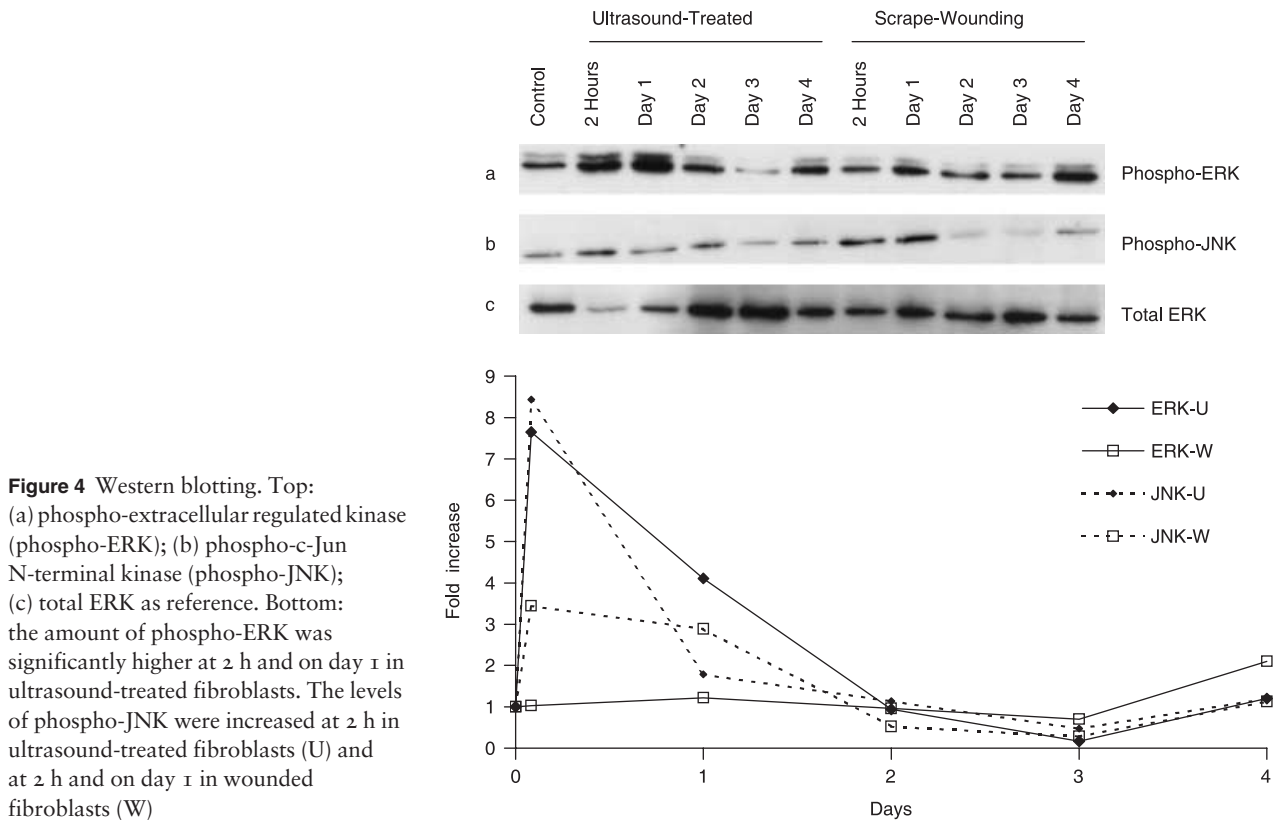


**Figure 5** Extracellular regulated kinase/c-Jun N-terminal kinase (ERK/JNK) ratio. The ERK/JNK ratio was increased early in ultrasound-treated fibroblasts and late in wounded fibroblasts

channels may provide more detailed information on the mechanisms by which ultrasound mist induces cellular responses.

This ultrasound mist system uses two ultrasonic effects to generate and propel the therapeutic mist towards the wound. The first effect is ultrasonic atomization, sometimes referred to as nebulization. This is similar to ultrasonic humidifiers. The saline solution which is applied to the metal face is atomized through vibration of the surface. This vibration causes

cavitation in the fluid, breaking it apart into small particles of well-controlled size. Once the particles of fluid are released from the tip, a second phenomenon drives them away and towards the wound. This second phenomenon is called acoustic streaming, or acoustic radiation force. At higher pressure levels, the traveling acoustic wave actually imparts a net force on the propagation medium, in this case the air. The force is sufficient to drive the particles of fluid along with it.

## Conclusion

On the basis of these and other observations, ultrasound seems to be a promising modality for wound healing. Nevertheless, further investigation of the expression of cytokine genes, cellular membrane effects, and cellular regenerative outcomes may better demonstrate the effects of ultrasound and predict the clinical efficacy of ultrasound on chronic wounds. We theorize that ultrasound waves from atomization and acoustic streaming vibrate the impacted cell membrane and create mechanical stimulation that initiates intracellular signaling networks.<sup>30,31</sup> Ultrasound mist therapy could also be applied to wound beds, where sharp debridement is not applicable, to promote stromal and epithelial regeneration.

## Acknowledgments

This project was supported by Celleration, Inc., Eden Prairie, MN, and the National Institutes of Health (NIH) grant T32 HD 07447. The authors wish to thank Karen Squillace for technical support.

## References

- Association AD. Economic costs of diabetes in the U.S. in 2002. *Diabetes Care* 2003; 26: 917–932.
- Bloomgarden ZT. Neuropathy, information technology, cost of diabetes care, and epidemiology. *Diabetes Care* 1998; 21: 1198–1202.
- Bloomgarden ZT. Epidemiology and neuropathy. *Diabetes Care* 1998; 21: 2023–2027.
- Currie CJ. The epidemiology and cost of inpatient care for peripheral vascular disease, infection, neuropathy, and ulceration in diabetes. *Diabetes Care* 1998; 21: 42–48.
- Mehta SS. Determining an episode of care using claims data. Diabetic foot ulcer. *Diabetes Care* 1999; 22: 1110–1115.
- O'Brien JA. Direct medical costs of complications resulting from type 2 diabetes in the US. *Diabetes Care* 1998; 21: 1122–1128.
- Ollendorf DA. Potential economic benefits of lower-extremity amputation prevention strategies in diabetes. *Diabetes Care* 1998; 21: 1240–1245.
- Mancini L. The diabetic foot: epidemiology. *Rays* 1997; 22: 511–523.
- Angle N, Bergan JJ. Chronic venous ulcer. *Br Med J* 1997; 314: 1019–1023.
- Lindholm C, Bergsten A, Berglund E. Chronic wounds and nursing care. *J Wound Care* 1999; 8: 5–10.
- Eaglstein WH, Falanga V. Chronic wounds. *Surg Clin North Am* 1997; 77: 689–700.
- Johannsen F, Nyholm A, Karlsmark T. Ultrasound therapy in chronic leg ulceration: a meta-analysis. *Wound Repair Regeneration* 1998; 6: 121–126.
- Houghton PE, Campbell KE. Choosing an adjunctive therapy for the treatment of chronic wounds. *Ostomy/Wound Manage* 1999; 45: 43–52.
- DeDeyne P, K-Volders M. In vitro effects of therapeutic ultrasound on the nucleus of human fibroblasts. *Phys Ther* 1995; 75: 629–634.
- Young S, Dyson M. Macrophage responsiveness to therapeutic ultrasound. *Ultrasound Med Biol* 1990; 16: 809–816.
- Al-Karmi IS, Dinno MA, Stoltz DA, et al. Calcium and the effects of ultrasound on frog skin. *Ultrasound Med Biol* 1994; 20: 73–81.
- Dinno MA, Dyson M, Young SR, et al. The significance of membrane changes in the safe and effective use of therapeutic and diagnostic ultrasound. *Phys Med Biol* 1989; 34: 1543–1552.
- Mortimer AJ, Dyson M. The effects of therapeutic ultrasound on the nucleus of human fibroblasts. *Ultrasound Med Biol* 1988; 14: 499–506.
- Turner S, Powell E, Ng C. The effect of ultrasound on the healing of repaired cockerel tendon: is collagen cross-linkage a factor? *J Hand Surg* 1989; 14B: 428–433.
- El-Batouty M, El-Gindy M, El-Shawat X. Comparative evaluation of the effects of ultrasound and ultraviolet irradiation on tissue regeneration. *Scand J Rheumatol* 1986; 15: 381–386.
- Dyson M. The effect of ultrasound on the rate of wound healing and the quality of scar tissue. In: *International Symposium on Therapeutic Ultrasound, Winnipeg, 1981*.
- Jackson BA, Schane JA, Starcher BC. Effect of ultrasound therapy on the repair of Achilles tendon injuries in rats. *Med Sci Sports Exercise* 1989; 23: 171–176.
- Webster DF, Harvey W, Dyson M, et al. The in vitro stimulation of collagen synthesis in human fibroblasts by ultrasound induced cavitation. *Ultrasonics* 1980; 16: 33.
- Byl NN, McKenzie AL, Wong T, et al. Incisional wound healing: a controlled study of low and high dose ultrasound. *J Orthop Sports Phys Ther* 1993; 18: 619–628.
- Baker KG, Robertson VJ, Duck FA. A review of therapeutic ultrasound: biophysical effects. *Phys Ther* 2001; 81: 1351–1358.
- Flemming K, Cullum N. Therapeutic ultrasound for pressure sores. *Cochrane Database Syst Rev* 2000; 4.
- Flemming K, Cullum N. Therapeutic ultrasound for venous leg ulcers. *Cochrane Database Syst Rev* 2000; 4.
- ter Haar G. Therapeutic ultrasound. *Eur J Ultrasound* 1999; 9: 3–9.
- Maxwell L, Collecutt T, Gledhill M, et al. The augmentation of leucocyte adhesion to endothelium by therapeutic ultrasound. *Ultrasound Med Biol* 1994; 20: 383–390.
- Chen K-D, Li Y-S, Kim M, et al. Mechanotransduction in response to shear stress. *J Biol Chem* 1999; 274: 18 393–18 400.
- Bogoyevitch MA, Ketterman AJ, Sugden PH. Cellular stresses differentially activate c-Jun N-terminal protein kinases and extracellular signal-regulated protein kinases in cultured ventricular myocytes. *J Biol Chem* 1995; 270: 29 710–29 717.
- Peus D, Vasa RA, Beyerle A, et al. UVB activates ERK1/2 and p38 signaling pathways via reactive oxygen species in cultured keratinocytes. *J Invest Dermatol* 1999; 112: 751–756.
- Peus D, Meves A, Vasa RA, et al. H<sub>2</sub>O<sub>2</sub> is required for UVB-induced EGF receptor and downstream signaling pathway activation. *Free Radic Biol Med* 1999; 27: 1197–1202.
- Peus D, Vasa RA, Meves A, et al. H<sub>2</sub>O<sub>2</sub> is an important mediator of UVB-induced EGF-receptor phosphorylation in cultured keratinocytes. *J Invest Dermatol* 1998; 110: 966–971.
- Pittelkow MR. Growth factors in cutaneous biology and disease. *Adv Dermatol* 1992; 7: 55–81.
- Coquette A, Berna N, Poumay Y, et al. The keratinocyte in cutaneous irritation and sensitization. In: Kydonieus AF, Wille JJ, eds. *Biochemical Modulation of Skin Reactions*. New York: CRC, 2000: 125–143.

- 37 Choquet D, Felsenfeld DP, Sheetz MP. Extracellular matrix rigidity causes strengthening of integrin-cytoskeleton linkages. *Cell* 1997; **88**: 39-48.
- 38 McDowell EM, Trump BF. Histologic fixatives suitable for diagnostic light and electron microscopy. *Arch Pathol Lab Med* 1976; **100**: 405-414.
- 39 Spurr AR. A low-viscosity epoxy resin embedding medium for electron microscopy. *J Ultrastruct Res* 1969; **26**: 31-43.
- 40 Peus D, Hamacher L, Pittelkow MR. EGF-receptor tyrosine kinase inhibition induces keratinocyte growth arrest and terminal differentiation. *J Invest Dermatol* 1997; **109**: 751-756.
- 41 Auclair M, Vigouroux C, Desbois-Mouthon C, *et al.* Antiinsulin receptor autoantibodies induce insulin receptors to constitutively associate with insulin receptor substrate-1 and -2 and cause severe cell resistance to both insulin and insulin-like growth factor I. *J Clin Endocrinol Metab* 1999; **84**: 3197-3206.
- 42 auf dem Keller U, Krampert M, Kumin A, *et al.* Keratinocyte growth factor: effects on keratinocytes and mechanisms of action. *Eur J Cell Biol* 2004; **83**: 607-612.
- 43 Brunner G, Blakytyn R. Extracellular regulation of TGF-beta activity in wound repair: growth factor latency as a sensor mechanism for injury. *Thromb Haemost* 2004; **92**: 253-261.
- 44 Wang J, Zheng H, Sung CC, *et al.* Cellular sources of transforming growth factor-beta isoforms in early and chronic radiation enteropathy. *Am J Pathol* 1998; **153**: 1531-1540.